The Effect of Rapid Rotation & Stratification on Homogeneous Turbulent Shear Flows via Linear Kinematic Simulations

Aaron Wienkers

1 Introduction

The evolution and statistics of developed turbulence quite often can dominate the resulting global system dynamics. This is especially the case for example in planetary boundary layers (atmospheric or oceanic) and astrophysical discs, where the structure of turbulence is influenced by the background shear, as well as system rotation and stable stratification. For example, the source and structure of turbulence in non-ionised Keplerian accretion discs (such as our very own nascent solar system) is still largely unknown [Johnson and Gammie, 2005], but is known to critically influence the protostellar accretion rate as well as the ability to seed planetesimal formation. It is thus desirable to understand more fully the exact turbulence suppression or enhancement mechanisms active in rotating and stratified homogeneous shear flows.

To this end, the structure and short-time evolution of turbulence in a rotating, stratified, and shearing domain will be studied via Rapid Distortion Theory (RDT) [Batchelor and Proudman, 1954]. Even though turbulence is inherently nonlinear, the linearisation proposed by Batchelor can still give useful insight into the behaviour of turbulence unrelated to the cascade. Distinct from conventional linear stability analysis which considers the exponential growth of a single eigenmode, but whose end result is quite often turbulence, the objective of RDT is to capture the short-time evolution of this resulting turbulence. It thus effectively forms a link between linear stability analysis and the behaviour of developed turbulence. RDT may also be utilised to motivate construction of turbulence models; however, the scope of this paper will be restricted to the trends of either stabilisation or destabilisation of turbulent fluctuations.

In particular, the evolution of turbulent fluctuations will be studied in a domain where the axis of rotation, shear, and stratification are *aligned*, as is often approximated in the atmospheric boundary layer. Deissler [1961] was the first to apply the ideas of RDT to study turbulence in plane shear flows. Similarly, Hanazaki and Hunt [2004] considered the effects of stable stratification on the spectrum of turbulence. Finally, Salhi and Cambon [2006] has explored particular analytic solutions to the RDT equations for the combined rotating, shearing, and stratified flows for the case with no streamwise fluctuations. Still much is yet unexplored for the evolution of 3D isotropic fluctuations in this situation where the axes of rotation and stratification are parallel. Nonetheless, many studies have used kinematic simulations (KS) of the RDT equations to evolve the case with these axes oriented perpendicular to each other (cf. Sagaut and Cambon [2008]), and so will be used as guidance.

2 Theoretical Model

2.1 Governing Equations

Assuming inviscid flow in a rotating frame, $\Omega\delta_{i3}$, the Boussinesq equations are

$$\begin{aligned} \frac{\partial \mathbf{u}}{\partial t} + (\mathbf{u}\cdot\nabla)\mathbf{u} + 2\boldsymbol{\Omega}\times\mathbf{u} &= -\frac{1}{\rho_0}\nabla p + b\mathbf{u} \\ \frac{\partial b}{\partial t} + (\mathbf{u}\cdot\nabla)b &= 0 \\ \nabla\cdot\mathbf{u} &= 0 \end{aligned} \tag{1}$$

where b is the local buoyancy which is coupled to the momentum equation via the background stratification. The desired mean vertical shear flow, $U_1 = Sx_3$, and the background buoyancy stratification, $\partial_3 B = -N^2$, however, are not a solution to (1). Thus, in order to linearise about this background state, we must make the typical geostrophic adjustment to balance the mean horizontal vorticity with a requisite component of stratification,

$$\partial_2 B = 2S\Omega. \tag{2}$$

The set (1) may then be linearised about this modified background state to give,

$$\begin{aligned} \partial_t u_i' + Sx_3\partial_1 u_i' + Su_3'\delta_{i1} + fu_j'\epsilon_{i3j} &= -\frac{1}{\rho_0}\partial_i p' + b'\delta_{i3} \\ \partial_t b + Sx_3\partial_1 b' + N^2\left(u_3' - \eta u_2'\right) &= 0 \\ \partial_i u_i' &= 0, \end{aligned} \tag{3}$$

where $\eta \equiv Sf/N^2$ is the isopycnal slope arising from the geostrophic correction, and $f \equiv 2\Omega$ is the Coriolis parameter.

2.2 RDT Formulation

The RDT equations for (3) may be found by expanding in the Kelvin modes [Craik and Criminale, 1986],

$$\begin{aligned} u_i' &= \hat{u}_i(t)\exp(-\mathrm{i}\kappa_j(t)x_j) + c.c. \\ b' &= \hat{b}(t)\exp(-\mathrm{i}\kappa_j(t)x_j) + c.c., \end{aligned} \tag{4}$$

where wavenumber, κ_i is allowed to vary in time, chosen for convenience to be governed by

$$\mathrm{d}_t\kappa_i + S\kappa_i\delta_{i3} = 0. \tag{5}$$

The governing equations (3) then become a system of ODEs in Lagrange-Fourier space,

$$\begin{aligned} \mathrm{d}_t\hat{u}_i &= S\hat{u}_3\delta_{i1} - f\hat{u}_j\epsilon_{i3j} + \frac{\mathrm{i}\kappa_i}{\rho_0}\hat{p} + \hat{b}\delta_{i3} \\ \mathrm{d}_t\hat{b} &= -N^2\left(\hat{u}_3 - \eta\hat{u}_2\right) \\ \hat{u}_i\kappa_i &= 0, \end{aligned} \tag{6}$$

where to eliminate pressure, the momentum equation may be projected onto the plane perpendicular to κ_i.

At this point, we can nondimensionalise the governing equations using S^{-1} as the unit of time, and the initial spectrum correlation length, $\mathcal{L}$, as the unit of length. Thus the background parameters

are $Ro \equiv S/f$ and $Ri \equiv N^2/S^2$, so that $\eta = (RoRi)^{-1}$. The nondimensional RDT equations are then

$$\begin{aligned}
\mathrm{d}_t \hat{u}_i &= -\left\{\delta_{i1} - 2\frac{\kappa_i\kappa_1}{\kappa^2}\right\}\hat{u}_3 - \frac{1}{Ro}\left\{\delta_{ij} - \frac{\kappa_i\kappa_j}{\kappa^2}\right\}\hat{u}_k \epsilon j3k + \left\{\delta_{i3} - \frac{\kappa_i\kappa_3}{\kappa^2}\right\}\hat{b} \\
\mathrm{d}_t \hat{b} &= -Ri\hat{u}_3 + \frac{1}{Ro}\hat{u}_2 \\
\kappa_1 &= \kappa_{1,0} \\
\kappa_2 &= \kappa_{2,0} \\
\kappa_3 &= \kappa_{3,0} - \kappa_{1,0}t,
\end{aligned} \tag{7}$$

where the Eikonal equations have been trivially solved exactly for this shearing flow.

This preceding analysis of dropping nonlinear rapid terms is valid so long as the turbulence is well-approximated as being frozen in time during deformation. This requires that

$$\frac{Sl_0}{u_0'} \gg 1, \tag{8}$$

or because of the convenient nondimensional units chosen which represent the energy containing scales at $\mathcal{L}^* = 1$ and $S^* = 1$, then $t \lesssim 1/u_0' \sim 10$.

3 Numerical Methods

Fung [1990] first introduced the idea of using Kinematic simulations to evolve the RDT equations in a non-deterministic framework, rather relying on statistical averaging to determine turbulent quantities of interest by evolving an ensemble of independent particles in Lagrange-Fourier space which together represent some initial turbulent spectrum. Each realisation of (7) solved is initialised from a stratified homogeneous isotropic turbulence spectrum. Due to the additional degree of freedom, the initial density fluctuations must also be specified. The von Karman kinetic energy spectrum is used for this purpose, which captures both the $E \propto k^4$ scale of the permanent eddies as well as the $E \propto k^{-5/3}$ slope in the inertial range. The spectrum is normalised such that the integral length is unity and the total energy is 1/2:

$$E(k) = 0.399\frac{k^4}{(0.5578 + k^2)^{17/6}}. \tag{9}$$

The initially randomly oriented, random phase, and logarithmically distributed wavenumbers are then used to sample the ensemble of $\hat{u}_{i,0}$ by

$$|\hat{u_i}|(\kappa_0) = \sqrt{2\int_{k-\delta k}^{k+\delta k} E(k)\ \mathrm{d}k}. \tag{10}$$

The buoyant energy is also sampled from a similar spectrum, but with a shallower k^2 spectrum at small wavenumbers [Chougule et al., 2013]. Here the integral length scale for TPE is set to be the same as TKE, although Gerz and Yamazaki [1993] have investigated in depth the effect of this buoyant length scale on the evolution of initial buoyancy perturbations (although the long-time behaviour is unchanged). This TPE spectrum is then

$$S(k) = 0.4274\frac{k^2}{(1.255 + k^2)^{11/6}}, \tag{11}$$

which is used to initialise $\hat{b}$ as

$$\hat{b}(\kappa_0) = \sqrt{Ri\int_{k-\delta k}^{k+\delta k} S(k)\ \mathrm{d}k}. \tag{12}$$

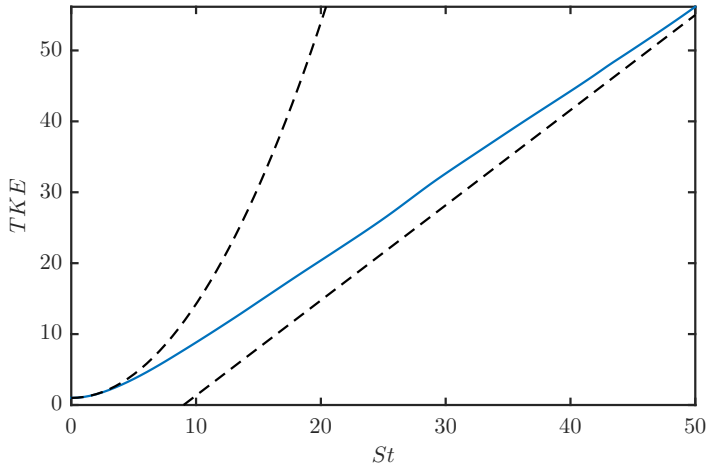

Figure 1: Comparison of TKE for numerical RDT solution with asymptotic solutions for pure shear ($Ri = 0$ and $Ro = \infty$).

Thus we may finally evolve each of the $N = 6400$ decoupled wave particles forward in time using a 4^{th} order Runge-Kutta numerical integration scheme. Further, because $\kappa_i(t)$ is known exactly, the divergence may be projected out of the solution after each step to improve accuracy.

4 Results

4.1 Homogeneous Shear Flow

According to the Rayleigh inflection point criterion, linear shear flow is linearly stable to exponentially growing modes. RDT does not assume this temporal structure, and in fact finds algebraic growth in line with experiments even though this is a linearised analysis! Indeed, if considering each mode individually, some may be growing, and some may be decaying, yet they average out to linear growth.

To help validate this RDT KS implementation, these initial results for homogeneous shear ($Ri = 0$ and $Ro = \infty$) are compared against the short- and long-time asymptotic solutions by Towsend [1970] and Moffatt [1967], respectively, and shown in Figure 1. The long-time behaviour may be understood after a few important observations. First, it is apparent from the Eikonal relations in equation (7) that the shear acts to right the wavenumbers vertically. Thus the turbulent structures become elongated in the stream-wise direction, which tends towards concentrating all fluctuation energy in R_{11}. Indeed, because wavevectors with small k_1 are less distorted by the shear, then the energy must be dominated by the small k_1 velocity components. Setting $k_1 = 0$, we see that (7) simplifies to

$$\mathrm{d}_t \hat{u}_1 = -\hat{u}_3, \tag{13}$$

recovering the linear growth at late times apparent in Figure 1.

This generic behaviour in shear flows is responsible for the formation of streaks prevalent in most free- and wall-bounded shear flows, and more specifically may be responsible for the formation of zonal jets and flows. This evolution is summarised by the evolution of the Lumley invariants in Figure 2. From the initial isotropy, the turbulence evolves nearly axisymmetrically with $\xi < 0$, i.e. towards the two-component limit. At intermediate times, the structures become two-component

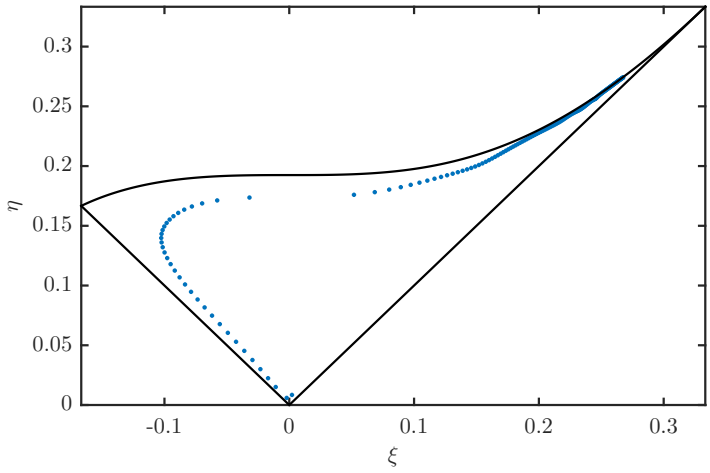

Figure 2: Lumley diagram showing the evolution of the Lumley invariants from isotropy for pure shear ($Ri = 0$ and $Ro = \infty$). Each dot is spaced $St/10$ apart.

axisymmetric with $\langle w'w' \rangle \approx 0$, before departing and asymptoting to the one-component limit as $\langle u'u' \rangle$ grows unbounded, forming streaks.

4.2 Stratified Shear Flow

4.2.1 Introduction

With the introduction of background stratification and the additional buoyancy equation, an additional eigensolution arises corresponding with internal gravity waves, which oscillate with the buoyancy frequency, N. Although internal gravity waves are activated by vertical fluctuations, it will become apparent that their influence on the energy growth is a bit more circuitous. First, as a reminder of the relevant energy transfer terms in stratified shear flow, the (nondimensional) TKE generation due to the background shear in this case is $P_k = -\langle u'w' \rangle$. Also, the buoyancy sink of momentum from the TKE equations is $S_k = Ri \langle u'b' \rangle$, which balances the source into the turbulent potential energy (TPE), $S_p = -\langle u'b' \rangle$. This conversion arises due to the anisotropic dispersion relation for internal gravity waves, which is preferentially vertical.

4.2.2 Validation

Linear stability analysis agrees with the experimental result that a subcritical instability exists, appearing at $Ri = 1/4$. It is thus encouraging that in the short-time limit, this RDT KS solution agrees with this result, and that *each* velocity component indeed decays (at least initially) in time. Of course, beyond $t = 0$, the analogy to conventional linear stability breaks, because this analysis is dynamical. In other words, although there are no nonlinearities modelled here, after $t = 0$, there still exists feedback mechanisms not captured in traditional linear stability analysis, and which may either generate or convert TKE.

4.2.3 Energy Exchange

The stabilisation by stratification may be understood by looking at the flow of energy through the system. As seen in Figure 4, initial production of the TKE by the shear is equivalent to the unstratified case. However, at the same time, energy is converted from TKE into TPE. Consequently,

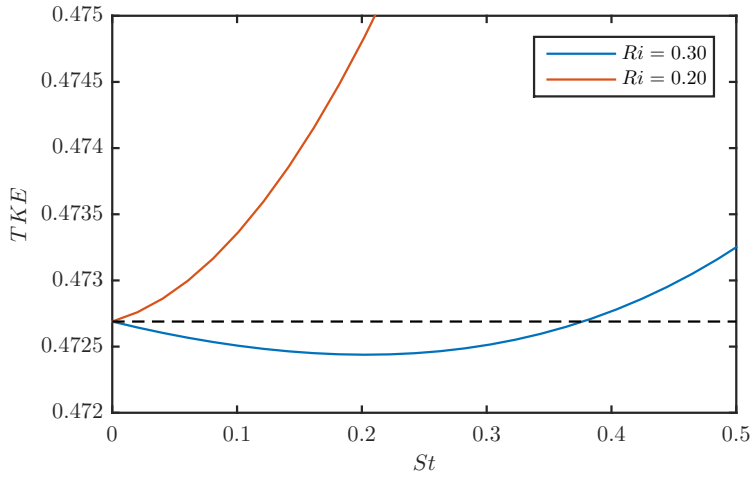

Figure 3: Analogous linear stability result verifying the $Ri_{\text{crit}} = 1/4$ is captured. Note the initial slope of TKE for the stable vs. unstable case.

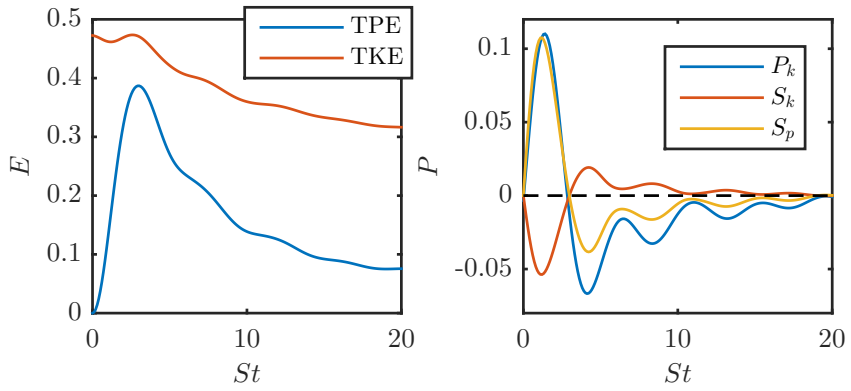

Figure 4: TKE and TPE evolution for $Ri = 0.5$, along with the relevant transfer quantities.

(since here no buoyancy perturbation is prescribed) there is some overshoot which sets up gravity wave oscillations with a period of $\tau_g = \pi/\sqrt{Ri} \approx 4.5$. However, eventually as the eddies again become two-component axisymmetric, the persistently positive R_{13} means that there is negative production (suppression) of TKE at long times, and the turbulent fluctuations decay away.

The TPE may be thought of as an available potential energy, but of course the linearised RDT cannot capture nonlinear mixing effects. In other words, because the background buoyancy is not evolving, there is no transfer from this available potential energy into background potential energy. Nonetheless, this is only expected to become important for long times or for very energetic turbulence.

4.2.4 Influence on Eddy Structure

We will now explore the effect of increasing stratification on the evolution of the eddy structure. The initial stratification-independent evolution towards two-component axisymmetric structure is apparent for every Ri, before feeling the tendency of the shear to drive towards one-component in

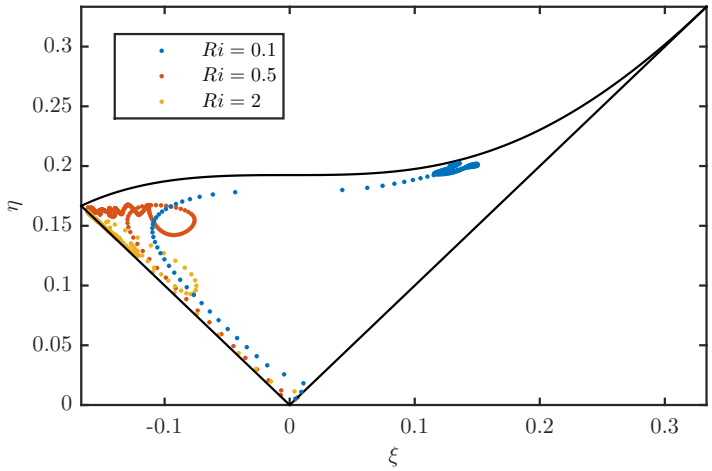

Figure 5: Lumley invariant diagram shown up to $St = 50$. Each dot is spaced $St/10$ apart.

the stream-wise direction. However, with increasing stratification the departure to one-component turbulence is inhibited. In particular, it is found that for $Ri \lesssim 0.3$ the turbulence oscillates near the two-component elliptical curve, rather than approaching the two-component limit.

A similar and equally critical change is also observed in the TKE production term for $Ri \gtrsim 0.3$ which has implications for the stabilisation of shear turbulence by stratification. As apparent in Figure 6, only above $Ri \sim 0.3$ does the shear production of TKE remain negative after the initial transient, and so the turbulence damps away, suppressed by the stratification. This is in agreement with the observation by Hanazaki and Hunt [2004]. Thus, the change in the eddy structure from one-component to two-component axisymmetric sees a reduction in the possible TKE production.

4.3 Rotating Shear Flow

Rotation by itself does not distort the spectrum of isotropic turbulence, and is therefore alone uninteresting. However, rotation is capable of modifying the anisotropic spectrum, say from a background shear, and so will briefly be considered here.

Analogously to the validation for stratified shear flow, we can build confidence in the implementation of the Coriolis source terms by checking against the known supercritical instability occurring at $Ro = 55$. The results for slightly sub- and super-critical Ro are given in Figure 7. In this case, however, there is no additional field to divert energy into. Rather, rotation suppresses turbulence by moving energy between components, via the pressure-strain term.

Two distinct asymptotic limits exist for $Ro \lessgtr 1$. For $Ro > 1$, where the shear is dominant, quite similar behaviour is observed as in §4.1. In particular, the shear dictates the evolution of the turbulent structure, and so the two-component axisymmetric turbulence gives way to eventual one-component turbulence ($\langle u'u' \rangle$) with streaks in the stream-wise direction. Now for $Ro < 1$, the dominant rotation is initially powerless to affect the isotropic turbulence. As rotation itself cannot generate anisotropy, the shear must first begin to generate one-component stream-wise structure before the rotation can prey off of the anisotropy. Thus, as evidenced in Figure 8, shortly after anisotropy is introduced, the rotation drives the turbulence to the one-component limit. However, rather than the principal eigenvector being oriented in the stream-wise direction, vertical columnar structures ($\langle w'w' \rangle$) form, akin to the classic Taylor columns.

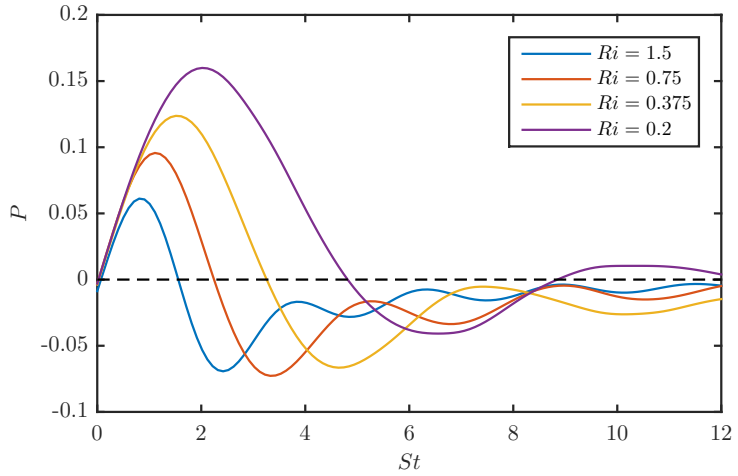

Figure 6: Shear production of TKE shown for various Ri.

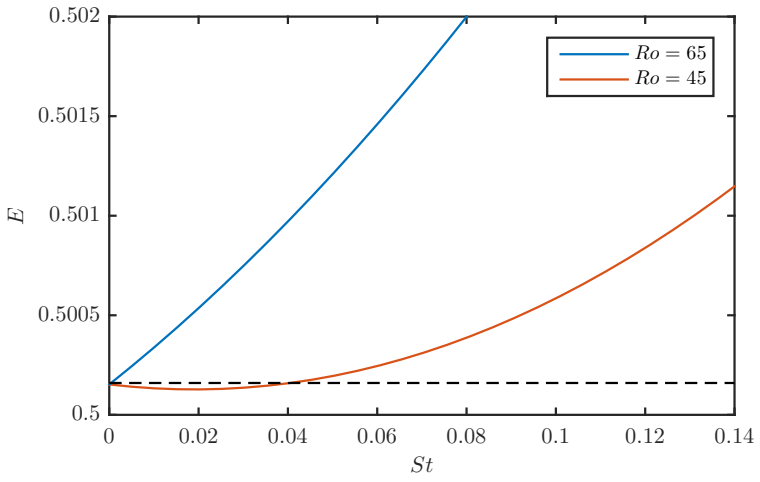

Figure 7: Analogous linear stability result verifying the $Ro_{\text{crit}} = 55$ is captured. Note the initial slope of TKE for the stable vs. unstable case.

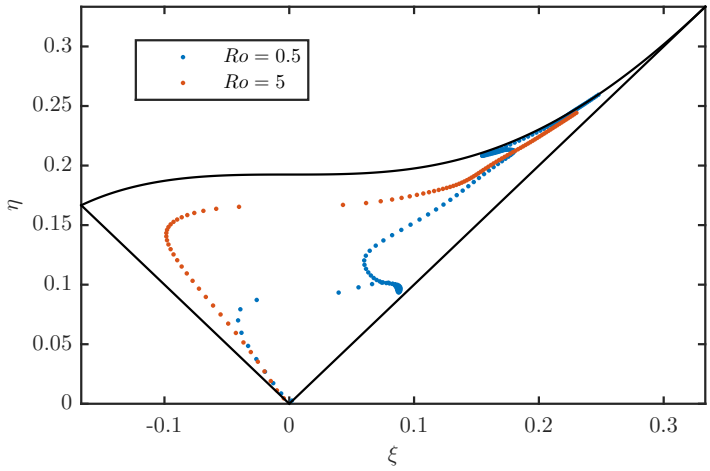

Figure 8: Lumley invariant diagram shown up to $St = 15$ each for a shear- and rotation-dominated flow. The $Ro = 5$ case asymptotes to one-component in the stream-wise direction, whereas for $Ro = 0.5$, the turbulence is in the one-component vertical limit. Each dot is spaced $St/10$ apart.

4.4 Rotating & Stratified Shear Flow

We can finally consider the more interesting case of combined rotation, stratification, and shear. With both rotation and stratification, the isopycnal tilt angle, η, from the geostrophic correction is no longer 0, which now sets the stage for a baroclinic instability. Salhi and Cambon [2006] have shown that in the limit $k_1 = 0$, the RDT formulation reduces to the linear stability bounds of this baroclinic instability. The neutral stability diagram in Ri-θ space is reproduced here in Figure 9, where θ is the angle the wavevector makes with the vertical. This shows that now for *any* $Ri < 1$, and finite Ro, there exists an unstable wavenumber with $k_1 \to 0$. Thus by simply introducing a slight system rotation, an initial turbulent spectrum will contain at least a few small-k_1 linearly unstable modes, which will affect the long-time asymptotic behaviour of the RDT results.

5 Conclusion and Learning Points

It is only by learning more about the linear processes that we can begin to understand the intricacies contained in the nonlinearities of the Navier-Stokes equations. Throughout this paper, an intuition has been developed, not only for the mechanisms and linear effects of rotation and stratification in suppression of turbulence, but also for the advantages and limitations of RDT as well as numerical kinematic simulations for approaching these problems. Rapid distortion theory in particular is just one method of extending the techniques of linear stability analysis to the evolution of turbulence. In recreating and extending the results of Salhi and Cambon [2006] for rotating and stratified homogeneous shear flows in this work, I have made a case for the utility of RDT in exploring the general landscape of a turbulent parameter space before investigating with expensive nonlinear simulations. In particular, as linear stability analysis has no jurisdiction over the dynamic evolution of turbulence, it is only with the extension of RDT that the suppression of shear-generated turbulence by stratification could be explained within this linear framework.

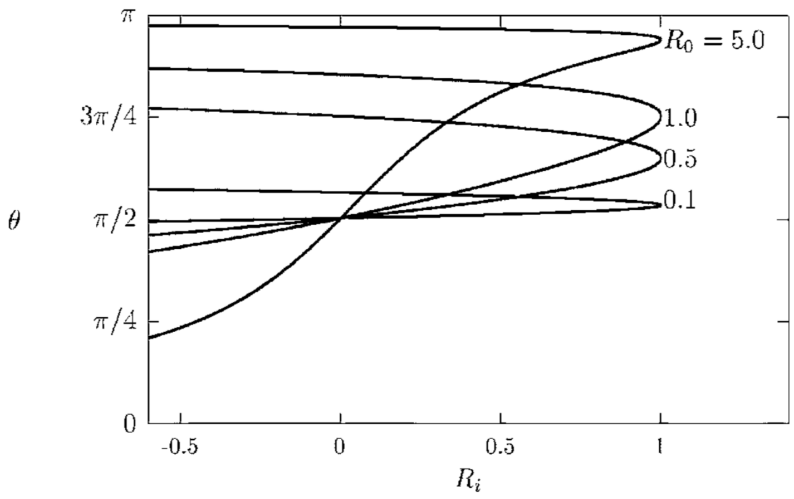

Figure 9: Neutral stability curves for baroclinic instability at various values for *Ro*. Shown here reproduced from Salhi and Cambon [2006].

References

G. K. Batchelor and I. Proudman. The Effect Of Rapid Distortion Of A Fluid In Turbulent Motion. *The Quarterly Journal of Mechanics and Applied Mathematics*, 7(1):83–103, 1954.

A. S. Chougule, J. Mann, and M. C. Kelly. Infulence of atmospheric stability on the spatial structure of turbulence. 2013.

A. D. D. Craik and W. O. Criminale. Evolution of Wavelike Disturbances in Shear Flows: A Class of Exact Solutions of the Navier-Stokes Equations. *Proceedings of the Royal Society A: Mathematical, Physical and Engineering Science*, 406(1830):13–26, July 1986.

R. G. Deissler. Effects of Inhomogeneity and of Shear Flow in Weak Turbulent Fields. *Physics of Fluids*, 4(10):1187, 1961.

J. C. H. Fung. *Kinematic simulation of turbulent flow and particle motions*. PhD thesis, Defense Technical Information Center, Fort Belvoir, VA, 1990.

T. Gerz and H. Yamazaki. Direct numerical simulation of buoyancy-driven turbulence in stably stratified fluid. *Journal of Fluid Mechanics*, 249(-1):415–440, Apr. 1993.

H. Hanazaki and J. Hunt. Structure of unsteady stably stratified turbulence with mean shear. *Journal of Fluid Mechanics*, 507:1–42, 2004.

B. M. Johnson and C. F. Gammie. Linear theory of thin, radially-stratified disks. *The Astrophysical Journal*, 626(2):978–990, 2005.

P. Sagaut and C. Cambon. *Homogeneous Turbulence Dynamics*. Cambridge University Press, June 2008.

A. Salhi and C. Cambon. Advances in Rapid Distortion Theory: From Rotating Shear Flows to the Baroclinic Instability. *Journal of Applied Mechanics*, 73(3):449–12, 2006.